

# Absorption and Attenuation in Soft Tissues: I—Calibration and Error Analyses

KEVIN J. PARKER, SENIOR MEMBER, IEEE, AND MARK E. LYONS

**Abstract**—Error estimations are developed for pulse decay absorption and radiation force insertion loss attenuation measurements. In absorption measurements, significant difficulty lies with accurate determination of peak intensity, especially where sharply focused beams are utilized. An intensity calibration is developed based on radiation force measurement of total power and main lobe beam patterns, using embedded thermocouples and short bursts of ultrasound. The main lobe measurements are highly reproducible, but sidelobes (which heavily influence estimates of total power) are easily corrupted by noise. Thus a theoretical extension of the main lobe beam pattern to include sidelobes is utilized to estimate peak focal intensity. The theory is based on circular baffled piston sources with apodizing lenses, an ideal condition that was closely approximated in a specially constructed experimental apparatus. The approach enables estimates of peak intensity *in situ* with typical uncertainty of less than five percent and resulting absorption coefficient uncertainty of 10 percent. Similar analyses of attenuation measurement uncertainties show that errors of three percent or less are possible where repeated measurements of radiation force insertion loss are made on relatively homogeneous materials. Comparisons of accurate measurements of both attenuation and absorption coefficients of tissues enable a clearer understanding of the dominant mechanisms of ultrasound-tissue interaction.

## I. INTRODUCTION

THE UNDERLYING mechanisms of ultrasonic attenuation, absorption, and scattering and their magnitudes in soft tissue are of great relevance to imaging, hyperthermia, and tissue characterization. The ultrasonic absorption coefficient of a material characterizes the rate at which acoustic energy is converted to local heating, whereas the attenuation coefficient encompasses all loss mechanisms, including the scattering or redistribution of longitudinal waves. Accordingly, absorption can be measured using embedded thermocouples to register temperature rise, whereas attenuation can be measured using insertion loss techniques. Literature values of attenuation and absorption were commonly reported to differ by a factor of two or more [1]–[3], possibly implying a large contribution of scattering (of longitudinal waves) to total attenuation of tissues. However, reports in the 1970's demonstrated how attenuation measurements could be artificially elevated by phase cancellation effects [4] and the presence of bubbles in samples [5]. Also, absorption measurements were shown to be artificially lowered by the use

of narrow beamwidths for tissue heating [6]. Given the recognition of these sources of error, and the development of the pulse-decay technique [7], [8] that permits absorption measurements using narrow focused beams and small tissue samples, it is reasonable to expect some convergence of attenuation and absorption values. This report derives expressions for the uncertainties in attenuation estimates (using phase-insensitive radiation force insertion loss measurements [9]) and absorption (using pulse-decay techniques). Assumptions include linear acoustic propagation and tissue properties that are homogeneous, isotropic, and closely matched to water. In practice, the most difficult field parameter to characterize is the peak intensity of focused fields, which must be known precisely to estimate absorption. We develop a hybrid calibration technique that utilizes planar scanning (51- $\mu\text{m}$  thermocouple probes) to obtain main lobe beam shapes. Then, theory is applied to extrapolate to the sidelobes. Since the sidelobe energy is noise sensitive but strongly influences the integration of total intensity, a theoretical extrapolation is found to be more reliable than sidelobe measurements for fields produced by specially constructed, baffled piston sources with apodizing lenses. Given a reliable calibration of peak intensities, an error analysis is derived for pulse-decay absorption measurements, and typical parameters are applied to measurements of tissue properties in the 1–13-MHz frequency range. A similar error analysis for radiation force attenuation measurements is also developed and applied using typical values from relatively homogeneous samples such as liver tissue. A companion paper [10] describes the application of these techniques in phantom, liver, brain, and muscle tissue.

## II. ABSORPTION MEASUREMENTS

### A. Calibration of Peak Focal Intensity

Absorption coefficients are, in the plane wave approximation, derived from the heat generation rate per unit intensity in a material. Thus accurate intensity measurements are required for absorption estimates. When submillimeter focused beams are utilized in pulse-decay experiments, conventional methods for intensity or beam pattern measurements, such as sphere deflection [11], or hydrophone planar scanning [12], are unusable because the probe sizes typically exceed the focal beamwidths. Thus a new intensity calibration approach is required. A method was developed that relies on the most accurate and reproducible quantities available.

Manuscript received January 5, 1987; revised May 13, 1987. This work was supported by the National Science Foundation under Grant ECE-8643973.

The authors are with the Department of Electrical Engineering, The University of Rochester, Rochester, NY 14627.

IEEE Log Number 8718128.

- 1) Total acoustic output derived from radiation force on an absorber, as measured by an electronic microbalance.
- 2) Main lobe beam pattern as measured by embedded 51- $\mu\text{m}$  thermojunctions. Here, the temperature spikes resulting from short ( $< 80$  ms) pulses can be used to produce an intensity profile with resolution on the order of a few thermocouple diameters (0.1 mm).

However, determination of peak intensity requires measurement of acoustic power and the entire beam pattern, side lobes as well as main lobe. Since side lobe measurements are generally noise corrupted, the main lobe beam patterns were curve fit to theoretical expressions, using amplitude weighting to emphasize the accurate main lobe data. In effect, theory is utilized to fill in the uncertain but influential sidelobe data, thus permitting reliable estimates of peak intensity.

The beam pattern curve fit is based on an analysis of the transducer and lens combination. The acoustic lens, like an optical lens, can be called a Fourier device [13]. The focal beam pattern represents the Fourier transform of the source. If the acoustic field is produced by an ideal circular baffled piston, the intensity beam pattern in the focal region of the lens should have the shape of  $[J_1(r)/r]^2$  where  $J_1$  is a Bessel function of order 1,  $r$  is the radial distance, and the function is referred to as the "Bessinc." In practice, baffled ceramic 1-in-diameter transducers were focused using acrylic lenses, and beam patterns were found to lie between Gaussian and Bessinc functions, because attenuating lenses have the additional effect of apodizing the source. Fig. 1(a) is an illustration of the lens and the apodizing function derived using ray theory and the measured attenuation coefficient of acrylic. Fig. 1(b) shows how the lens apodizes the velocity function for different values of attenuation (frequency). As  $\alpha$  increases, the uniform velocity function approaches a Gaussian, which will Fourier transform to (thus focus to) a Gaussian intensity beam pattern. Therefore, the two extremes of the possible intensity profiles in the focal region are Gaussian and a Bessinc function. This provides the theoretical basis for our calibration of peak intensity.

Assume the focal intensity distribution is Gaussian given by

$$I(r) = I_0 e^{(-r^2/\beta)} \quad (1)$$

where  $\beta^{1/2}$  is a measure of beamwidth and  $I_0$  is the peak intensity. In this case the peak intensity can be simply derived from measurements of total acoustic power  $P_T$  and beamwidth  $\beta$ :

$$P_T = \int_0^{2\pi} \int_0^\infty I(r) \cdot r \, dr \, d\theta \quad (2)$$

$$P_T = 2\pi I_0 \int_0^\infty r e^{(-r^2/\beta)} \cdot dr, \quad (3)$$

thus

$$I_0 = \frac{P_T}{\pi\beta} \quad (4)$$

is the desired result, with  $P_T$  obtainable from radiation force and  $\beta$  derived from curve fit of measured intensity profiles.

Next, assume that an ideal Bessinc function with scale factor  $a$  describes focal intensity:

$$I(r) = I_0 \left[ \frac{2J_1(ar)}{ar} \right]^2. \quad (5)$$

If this Bessinc function is curve fit with amplitude weighting (to emphasize the fit in the main lobe) to a Gaussian, then as shown in Fig. 2, the weighted Gaussian fit essentially ignores energy in the sidelobes of the Bessinc, and therefore the use of (4) will result in an estimate of  $I_0$  which is approximately 13 percent too high. Extensive simulations of the two-dimensional (2D) Fourier transforms of the apodizing functions shown in Fig. 1(b) provided the following results. When this restricted class of beam patterns is curve fit with amplitude weighting to a Gaussian, the relationship between peak intensity, total power, and beamwidth is given by

$$I_0 = \frac{CP_T}{\pi\beta} \quad (6)$$

where

$$C = \begin{cases} 0.87, & \text{for } \alpha < 2 \text{ Np/cm;} \\ & \text{weakly apodized source} \\ 0.87 < C < 1, & \text{for } 2 < \alpha < 10 \text{ Np/cm;} \\ & \text{moderately apodized source.} \\ 1, & \text{for } \alpha > 10 \text{ Np/cm;} \\ & \text{highly apodized source} \end{cases}$$

Thus peak intensity can be estimated *in situ* using the same thermocouple in tissue to measure the beam pattern, as well as the rate of heating or pulse decay absorption experiment. This information, plus an independent measurement of total acoustic power (taken for practical reasons at a proximal plane then corrected for water attenuation to the focal plane) plus an estimate of the apodization function, are sufficient for determination of peak intensity.

Examples of measured beam patterns at 2 and 10 MHz are given in Fig. 3, with weighted Gaussian curve fits. A least-squares-error fit was used that fits the log of the data to a parabola, using weights proportional to the magnitude of the original data. The 2-MHz pattern shows evidence of sidelobes, whereas the 10-MHz beam pattern sidelobe information is hidden in noise. The use of higher intensities at 10 MHz would be desirable for increasing the signal-to-noise ratio in the sidelobe region but, in this configuration (8-cm focal length), would result in undesirable shock production. In both cases the lens attenua-

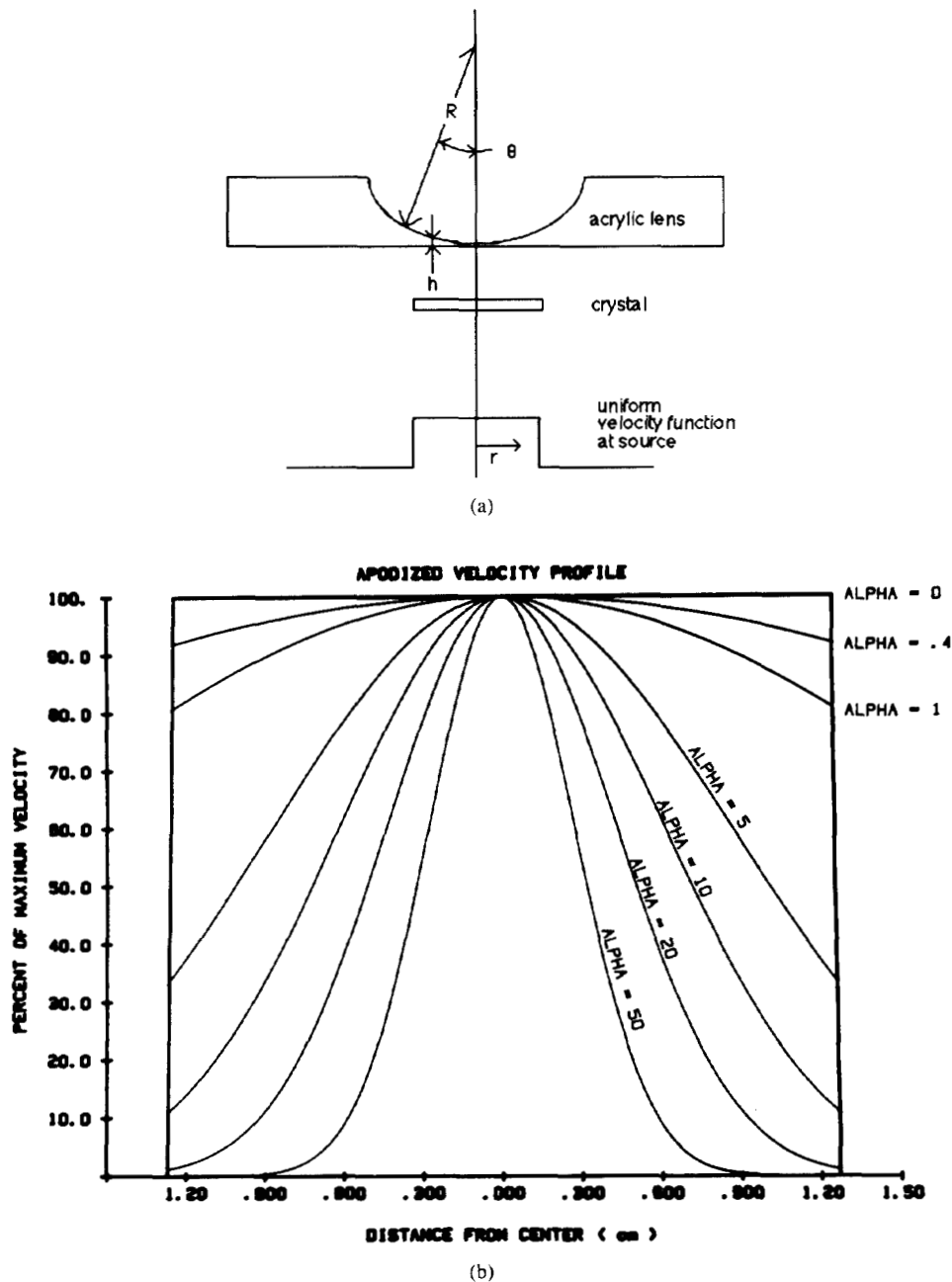


Fig. 1. (a) Ideal circular piston source focused and apodized by attenuating plastic lens. Ray tracing analysis yields the intensity as function of radial position just after lens. (b) Apodized velocity source function given ideal 1-in-diameter piston source and lens with radius of curvature  $R = 3.74$  cm, and various attenuation coefficients (ALPHA, Np/cm). High attenuation coefficients result in source functions that are nearly Gaussian.

tion  $\alpha$  is less than  $2 N_p/\text{cm}$ , so a value of  $C = 0.87$  would be used in (6) for determination of peak focal intensity.

While the technique mentioned is restricted to nearly ideal baffled apodized symmetric focused beams, it has been possible to construct and utilize a test facility that closely approximates these conditions [10]. The beams formed with and without lucite lenses were found to be symmetric, and the effective transducer diameters were nearly 100 percent of the piezoelectric disk diameters [15]. Comparisons were made of peak intensity estimated using

the new technique, against predictions from unapodized diffraction limited focusing theory [13], [14] and against sphere deflection estimates at low frequencies where broad beam patterns permit the use of a 1/16-in steel sphere. The new technique produced close agreement ( $< 10$  percent at 1 MHz) with these other estimates of peak intensity, providing initial validation of the approach.

The uncertainty in estimating peak intensity will be discussed in the next section, but a few comments are germane. Assuming that the acoustic model represents the experimental apparatus, the uncertainty of  $I_0$  can be made

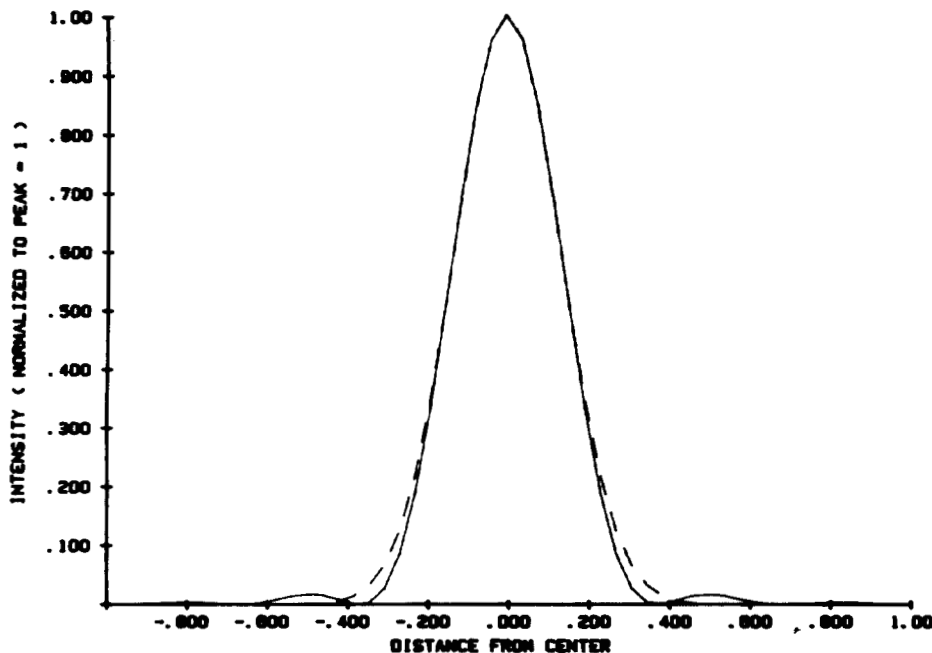


Fig. 2. Least-squares-error curve fit of Gaussian function (dashed) to Bessel (solid). Amplitude weighting is utilized to emphasize main lobe fit.

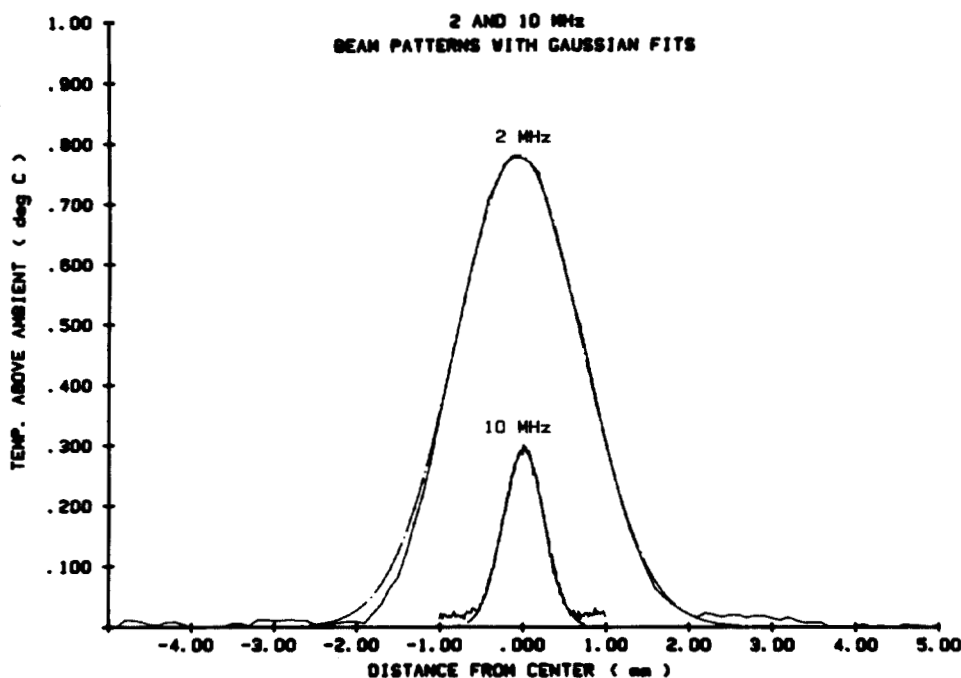


Fig. 3. Measured beam patterns at 2 and 10 MHz, with Gaussian curve fits. Data are measured from 51- $\mu$ m thermocouples in absorbing rubber compound. Short pulses ( $\leq 0.08$  s) of ultrasound result in temperature spikes that are proportional to intensity. Precision translator axis is used to scan probe across field.

quite low since total acoustic power can be determined accurately using a sensitive microbalance with averaging; main lobe measurements are highly reproducible using precision positioning axes and small thermocouple probes; and the constant  $C$ , which results from apodization, varies at most between 1 and 0.87, with much less variation over a restricted frequency range. In principle, accuracies of five percent or less are achievable, even in the case of submillimeter beamwidths.

*B. Error in Pulse Decay Absorption Estimates*

The form of sensitivity analysis for a general function of several variables  $f(x, y, z, \dots)$  is

$$\sigma_f^2 = \left(\frac{\partial f}{\partial x}\right)^2 \sigma_x^2 + \left(\frac{\partial f}{\partial y}\right)^2 \sigma_y^2 + \left(\frac{\partial f}{\partial z}\right)^2 \sigma_z^2 + \dots \quad (7)$$

In the case of the pulse decay model, the amplitude absorption coefficient  $\alpha$  is a function of several quantities which will either be assumed or measured [7], [8].

$$\alpha = \frac{T_{\text{exp}} \rho C \left[ 1 + \left( \frac{4kt}{\beta} \right) \right]}{I_0 \left[ 1 + \operatorname{erf} \left( \frac{z}{\sqrt{4kt}} \right) \right]} \exp \left[ \frac{r^2}{(4kt + \beta)} \right] \quad (8)$$

or

$$\alpha = f(T_{\text{exp}}, \rho, C, \beta, I_0, r, k, z, t) \quad (9)$$

where  $T_{\text{exp}}$  is the thermocouple measurement of temperature decay,  $\rho$ ,  $C$ , and  $k$  are the tissue density, specific heat, and thermal diffusivity,  $r$  is the radial separation between the thermocouple and the beam focal point, and  $z$  is the depth of the thermocouple in a semi-infinite sample. It is assumed that time  $t$  following the ultrasonic pulse is known with high precision and does not contribute to the uncertainty in attenuation.

Applying the general error expression to (8) yields

$$\begin{aligned} \sigma_{\alpha}^2 &= \left( \frac{\partial f}{\partial T_{\text{exp}}} \right)^2 \sigma_{T_{\text{exp}}}^2 + \left( \frac{\partial f}{\partial \rho} \right)^2 \sigma_{\rho}^2 \\ &+ \left( \frac{\partial f}{\partial C} \right)^2 \sigma_C^2 + \left( \frac{\partial f}{\partial \beta} \right)^2 \sigma_{\beta}^2 \\ &+ \left( \frac{\partial f}{\partial I_0} \right)^2 \sigma_{I_0}^2 + \left( \frac{\partial f}{\partial r} \right)^2 \sigma_r^2 \\ &+ \left( \frac{\partial f}{\partial k} \right)^2 \sigma_k^2 + \left( \frac{\partial f}{\partial z} \right)^2 \sigma_z^2. \end{aligned} \quad (10)$$

After applying partial terms to (8) and rearranging, we have

$$\begin{aligned} \left( \frac{\sigma_{\alpha}}{\alpha} \right)^2 &= \left( \frac{\sigma_{T_{\text{exp}}}}{T_{\text{exp}}} \right)^2 + \left( \frac{\sigma_{\rho}}{\rho} \right)^2 + \left( \frac{\sigma_C}{C} \right)^2 \\ &+ \left( \frac{\sigma_{\beta}}{\beta} \right)^2 \left[ \frac{-4kt \left( \frac{4kt}{\beta} + 1 \right) - r^2}{\beta \left( \frac{4kt}{\beta} + 1 \right)^2} \right]^2 \\ &+ \left( \frac{\sigma_{I_0}}{I_0} \right)^2 + \left( \frac{\sigma_r}{r} \right)^2 \left[ \frac{4r^4}{(4kt + \beta)^2} \right] \\ &+ \left( \frac{\sigma_k}{k} \right)^2 \left[ 16k^2 t^2 \left[ \frac{4kt + \beta - r^2}{(4kt + \beta)^2} \right]^2 \right] \\ &+ \left( \frac{\sigma_z}{z} \right)^2 \left[ \frac{z^2 H_0^2 \left( \frac{z}{\sqrt{4kt}} \right) \exp \left( \frac{-2z^2}{4kt} \right)}{4kt \left( 1 + \operatorname{erf} \left( \frac{z}{\sqrt{4kt}} \right) \right)^2} \right] \end{aligned} \quad (11)$$

where  $H_0$  is a Hankel function of 0th order, and the multiplier in  $\sigma_k$  term excludes an  $\operatorname{erf} [z/(4kt)^{1/2}]$  term because of the weak  $(kt)^{1/2}$  dependence. In terms of the

percent error of each term (percent  $E_x = \sigma_x/x$ ) we have

$$\begin{aligned} (\% E_{\alpha})^2 &= (\% E_{T_{\text{exp}}})^2 + (\% E_{\rho})^2 + (\% E_C)^2 \\ &+ (\% E_{\beta})^2 \left[ \frac{-4kt \left( \frac{4kt}{\beta} + 1 \right) - r^2}{\beta \left( \frac{4kt}{\beta} + 1 \right)^2} \right]^2 \\ &+ (\% E_{I_0})^2 + (\% E_r)^2 \left[ \frac{4r^4}{(4kt + \beta)^2} \right] \\ &+ (\% E_k)^2 \left[ 16k^2 t^2 \left[ \frac{4kt + \beta - r^2}{(4kt + \beta)^2} \right]^2 \right] \\ &+ \left( \frac{\sigma_z}{z} \right)^2 \left[ \frac{z^2 H_0^2 \left( \frac{z}{\sqrt{4kt}} \right) \exp \left( \frac{-2z^2}{4kt} \right)}{4kt \left( 1 + \operatorname{erf} \left( \frac{z}{\sqrt{4kt}} \right) \right)^2} \right]. \end{aligned} \quad (12)$$

Equation (12) shows the extent to which an error in any quantity will affect the error in  $\alpha$ . The multiplying factors in each term will either increase or decrease the significance of the particular error.

Equation (12) is a general sensitivity expression which includes all the terms in the pulse decay model. Of particular interest in the equation are the terms involving  $I_0$  and  $\beta$ . Recall from the previous section the method chosen to determine peak intensity in weakly apodized focused fields:

$$I_0 = \frac{P_T(0.87)}{\pi \beta}. \quad (13)$$

Therefore, the  $I_0$  dependence in the pulse decay model can be replaced with the two terms  $P_T$  and  $\beta$ .

Substituting (13) into (8) and applying differentiation results in a modified equation for error in  $\alpha$ :

$$\begin{aligned} (\% E_{\alpha})^2 &= (\% E_{T_{\text{exp}}})^2 + (\% E_{\rho})^2 + (\% E_C)^2 \\ &+ (\% E_{\beta})^2 \left[ \frac{4kt + \beta - r^2}{\beta \left( \frac{4kt}{\beta} + 1 \right)^2} \right]^2 \\ &+ (\% E_{P_T})^2 + (\% E_r)^2 \left[ \frac{4r^4}{(4kt + \beta)^2} \right] \\ &+ (\% E_k)^2 \left[ 16k^2 t^2 \left( \frac{4kt + \beta - r^2}{(4kt + \beta)^2} \right)^2 \right] \\ &+ (\% E_z)^2 \left[ \frac{z^2 H_0^2 \left( \frac{z}{\sqrt{4kt}} \right) \exp \left( \frac{-2z^2}{4kt} \right)}{4kt \left( 1 + \operatorname{erf} \left( \frac{z}{\sqrt{4kt}} \right) \right)^2} \right]. \end{aligned} \quad (14)$$

TABLE I  
COMPARISON OF ERROR MULTIPLIER FOR BETA TERM<sup>a</sup>

	Independent measurement of $I_0$	Calculation of $I_0$ Using $P_T$ and $\beta$
$\beta = 5 \times 10^{-2} \text{ cm}^2$ (~1 MHz)		
$r = 0$	0.14	0.39
$r = \sqrt{\beta}$	0.59	0.06
$r = 2\sqrt{\beta}$	3.70	0.88
$\beta = 3 \times 10^{-3} \text{ cm}^2$ (~5 MHz)		
$r = 0$	0.83	0.0083
$r = \sqrt{\beta}$	0.84	0.0068
$r = 2\sqrt{\beta}$	0.89	0.0033
$\beta = 1 \times 10^{-3} \text{ cm}^2$ (~12 MHz)		
$r = 0$	0.94	0.0010
$r = \sqrt{\beta}$	0.94	0.0010
$r = 2\sqrt{\beta}$	0.95	0.0008
$(k = 0.0015 \text{ cm}^2/\text{s}, t = 5 \text{ s}, \text{ all cases})$		
Beta error multiplier using independent $I_0$	Beta error multiplier using $P_T$ and $\beta$ to calculate $I_0$	
$\left[ \frac{1}{\beta} \left( \frac{4kt(4kt/\beta + 1) + r^2}{(4kt/\beta + 1)^2} \right) \right]^2$	$\left[ \frac{1}{\beta} \frac{(4kt + \beta - r^2)}{(4kt/\beta + 1)^2} \right]^2$	

<sup>a</sup>Sensitivity of pulse decay absorption to errors in beamwidth  $\beta^{1/2}$  is reduced when beamwidth is used to calculate peak intensity.

Equation (14) differs from the previous error equation in two terms. The term of  $I_0$  in the general case has been replaced with an identical term involving  $P_T$ . Also, the original multiplier of error in  $\beta$  has been altered.

Close examination of the new error equation shows that the error in  $\alpha$  is much less affected by any error in  $\beta$ , since deviation from true value affects both the numerator and intensity (denominator) of (8) in a nearly proportional manner. Table I shows this change in sensitivity when beamwidth is used to estimate peak intensity. The calculations were performed using representative values at different frequencies. This decreased sensitivity to  $\beta$  is one positive side effect of this method for the determination of peak intensity.

The error term involving uncertainty in total acoustic power is, in practice, frequency dependent. In experiments the total power applied drops with increasing frequency, as focusing provides greater gain, and higher attenuation produces greater heating. Thus, against a background of constant mechanical or vibrational noise, the error in radiation force power measurements will sharply increase with frequency. Fortunately, power measurements can be made repeatedly and averaged for each experiment. Statistical theory predicts that averaging can decrease the percent error in a measurement by  $N^{1/2}$ , where  $N$  is the number of samples taken. Therefore, experimental averaging can be used to reduce the total power percent error term. Fig. 4 shows the frequency dependence of the percent error in power for typical experiments [10] taken on axis ( $r = 0$ ) and off axis ( $r = \beta^{1/2}$ ,  $2\beta^{1/2}$  where higher powers are typically used). Representative power levels range from 3 W at low frequencies to 50 mW at 12 MHz, measured against a noise equivalent

of less than approximately 7 mW. With suitable averaging, the error can be held below 3 percent, even for high-frequency low-power experiments.

Fig. 4 also shows the frequency dependence of the multipliers for radius, thermal conductivity, and  $\beta$  percent error terms. The typical experimental values of beamwidths  $\beta$  were used in the expressions of (14). The product of these small multipliers with their respective percent errors (typically less than five percent) produces negligible contributions to the total error in absorption, except in the case of position ( $r$ ) uncertainty in far-off axis experiments ( $r = 2\beta^{1/2}$ ), at low frequencies.

The depth term  $z$  in (14) has a multiplier that is independent of frequency but varies with thermocouple depth as shown in Fig. 5. Again, typical parameters of  $k = 1.5 \times 10^{-3} \text{ cm}^2/\text{s}$  and  $t = 5 \text{ s}$  were used in the calculations, and the product of the small multiplier shown in Fig. 5 times a small (15 percent or less) uncertainty in thermocouple depth, produces an insignificant contribution to overall uncertainty. Finally, three terms of (14) ( $T_{\text{exp}}$ ,  $\rho$ , and  $C$ ) have no frequency dependence and no multiplier. A constant percent error of five percent was used to represent the uncertainty in thermocouple temperature reading,  $T_{\text{exp}}$  (including noise and calibration errors), and tissue density and specific heat (which approach values for water in tissues with high wet/dry weight ratios) [16]. When combined according to (14) with all other error terms, the final result is a relatively constant percent error in attenuation estimates of approximately ten percent, as shown in Fig. 6. Here,  $t = 5 \text{ s}$ ,  $k = 1.5 \times 10^{-3} \text{ cm}^2/\text{s}$ ,  $z = 2 \text{ mm}$  were used as typical parameters, and results for on- and off-axis experiments are shown. In practice, low-frequency off-axis ( $r = 2\beta^{1/2}$ )

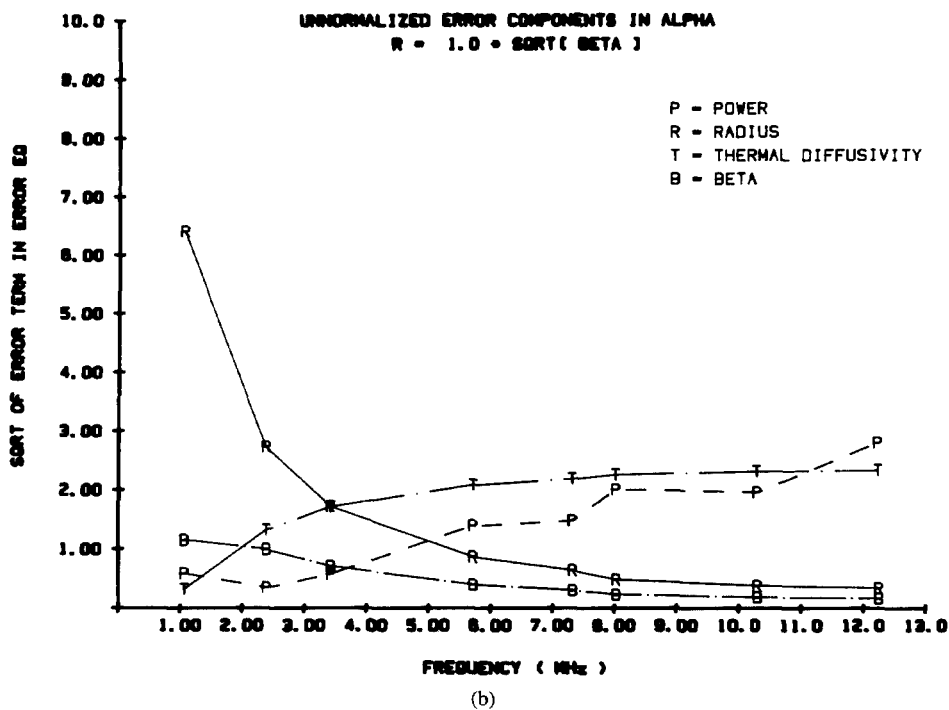
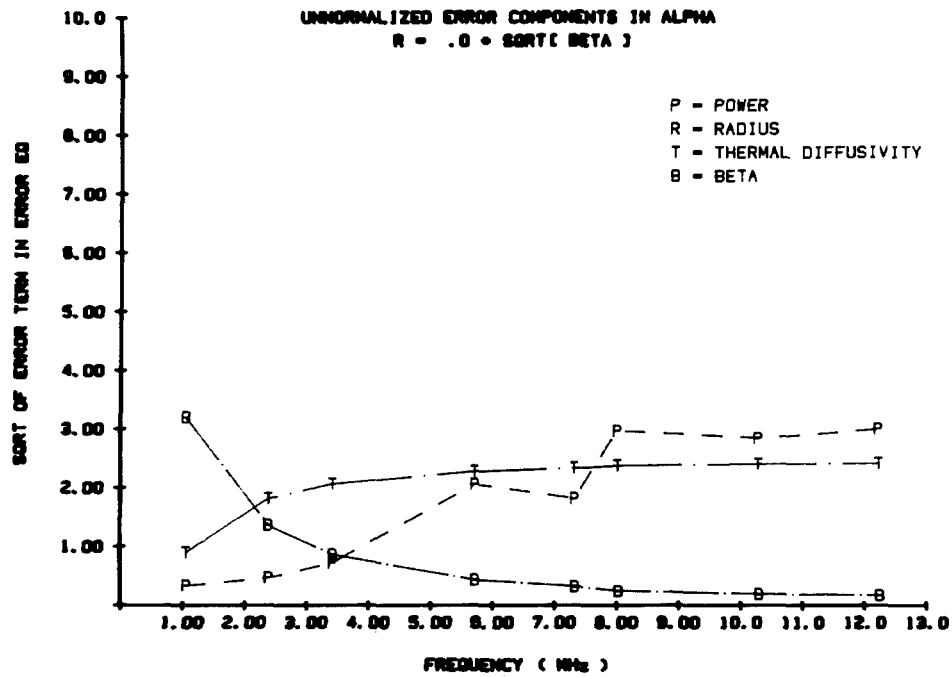


Fig. 4. Components of the absorption error equation, for on axis ( $r = 0$ ) and two off-axis ( $r = \beta^{1/2}$ ,  $2\beta^{1/2}$ ) pulse-decay experiments.  $P$  is the percent error in acoustic power measurements, obtained from actual experiments.  $R$ ,  $T$ , and  $B$  are square roots of multipliers of percent error in radius, thermal diffusivity, and beta, respectively. These three functions are calculated from sensitivity analysis of pulse-decay equation and are frequency dependent because they depend on beamwidth  $\beta$ , which sharply decreases with increasing frequency in our apparatus.

experiments were avoided because of the larger errors, and the practical complication of large displacements required by large beamwidths.

The principal contributing sources of errors are, there-

fore, from noise in power measurements, and uncertainty in tissue materials properties. Of these, the tissue-specific heat uncertainty is most problematic because it cannot be easily arrived at by the averaging of experimental values

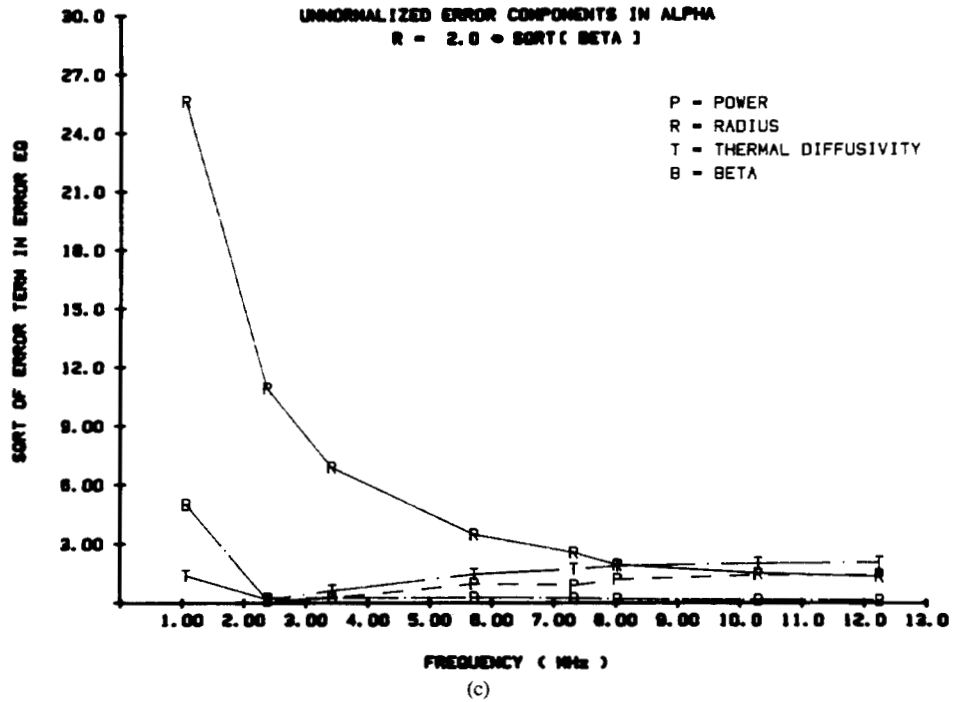


Fig. 4 (Continued)

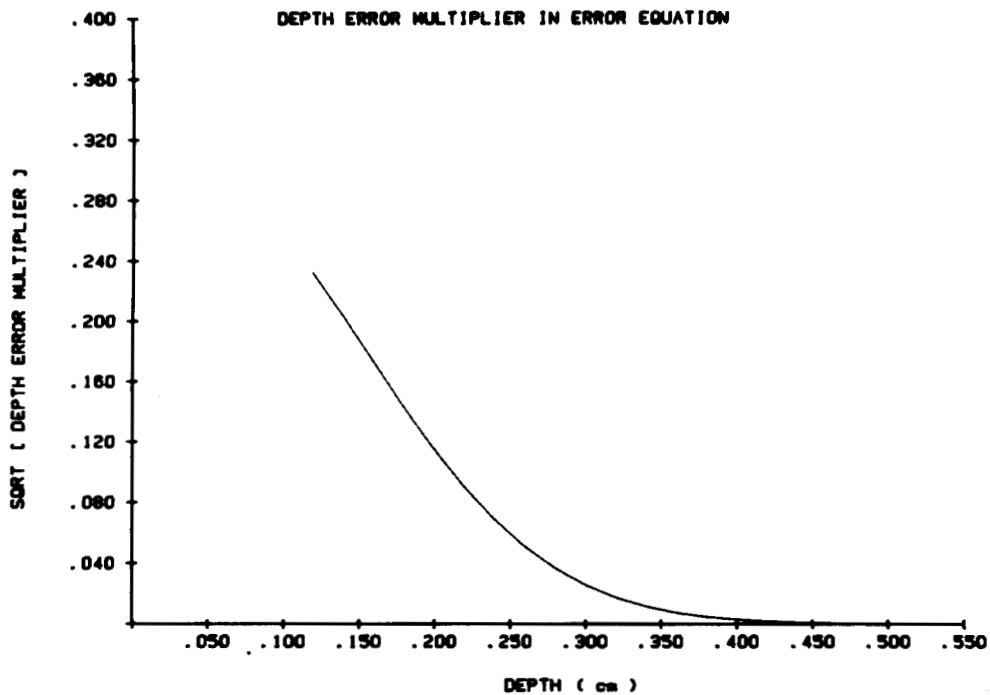


Fig. 5. Sensitivity of pulse decay absorption to uncertainties in thermocouple depth. Shown is square root of depth error multiplier, as function of thermocouple location. This term is frequency independent.

with zero mean error. Rather, a single value is typically assumed based on water specific heat, and any deviations of tissue from the assumed value will directly bias the absorption estimate. As better estimates of tissue density and specific heat become available, the uncertainty in absorption can drop to 7 percent over all frequencies, without further refinement of the experimental technique. The above discussions assume macroscopically homogeneous tissue samples. In the case of grossly inhomogeneous or

anisotropic tissues such as brain matter or hind leg muscle [10], additional variability will influence the measurements, and the basic models of beam absorption and heat diffusion may be compromised.

### III. ATTENUATION MEASUREMENTS

The use of radiation force insertion loss measurements for attenuation is conceptually and experimentally simpler than absorption measurements. In the former case, colli-

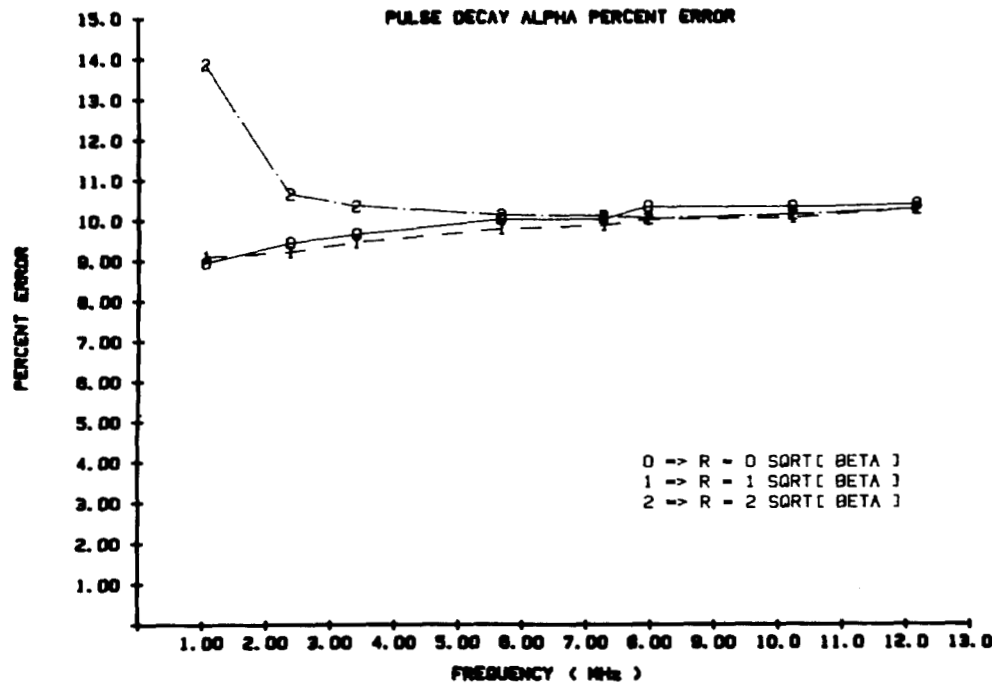


Fig. 6. Total-percent error in pulse-decay absorption measurements for on-axis ( $r = 0$ ) and off-axis ( $r = \beta^{1/2}, 2\beta^{1/2}$ ) experiments. Lower uncertainty would be possible with improved values for tissue density and specific heat.

mated beams may be used, eliminating alignment problems of the sample-thermocouple-focal point. A broad collimated beam provides spatial averaging, which is useful for inhomogeneous samples. When reflection artifacts are eliminated and parallel faced samples are introduced between the source and absorber, the insertion loss is given by

$$P_W = P_0 e^{-2Ad} \quad (15)$$

where  $P_W$  and  $P_0$  represent power with sample, and without sample, respectively,  $A$  is the amplitude attenuation coefficient of the material, and  $d$  the sample thickness. Thus

$$A = \frac{-\ln\left(\frac{P_W}{P_0}\right)}{2d} \quad (16)$$

provides the estimate of attenuation given acoustic power measurements. Since a power ratio is obtained, it is not necessary to utilize the radiation force constant of 67 mg/W for a normal perfectly absorbing radiation force "receiver."

Applying the general error expression to (16) yields

$$\sigma_A^2 = A^2 \left(\frac{\sigma_d}{d}\right)^2 + \left(\frac{1}{2d}\right)^2 \left[ \left(\frac{\sigma_{P_W}}{P_W}\right)^2 + \left(\frac{\sigma_{P_0}}{P_0}\right)^2 \right]. \quad (17)$$

Rearranging to form percent errors gives

$$(\% E_A)^2 = (\% E_d)^2 + \left(\frac{1}{2dA}\right)^2 [(\% E_{P_W})^2 + (\% E_{P_0})^2], \quad (18)$$

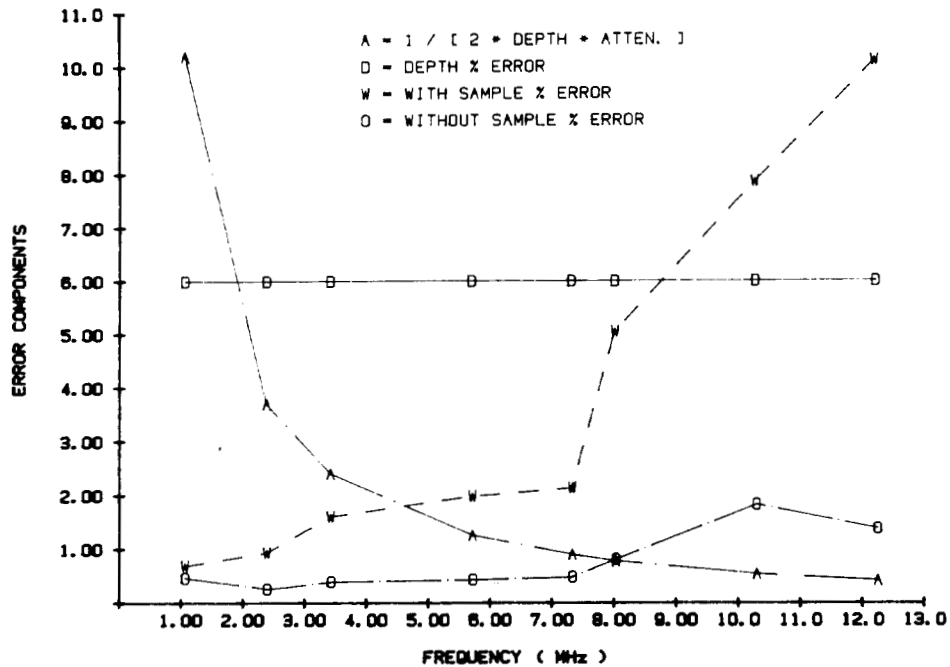
which is the desired result.

The evaluation of these terms as a function of thickness, attenuation, and frequency is not straightforward because of implicit and/or system-dependent relationships. For example, it would seem as if an increase in sample thickness  $d$  would monotonically decrease attenuation uncertainty. However, as sample thickness increases, power transmission drops exponentially, and as the receiver noise floor or resolution floor is approached the percent  $E_{P_W}$  term will increase sharply.

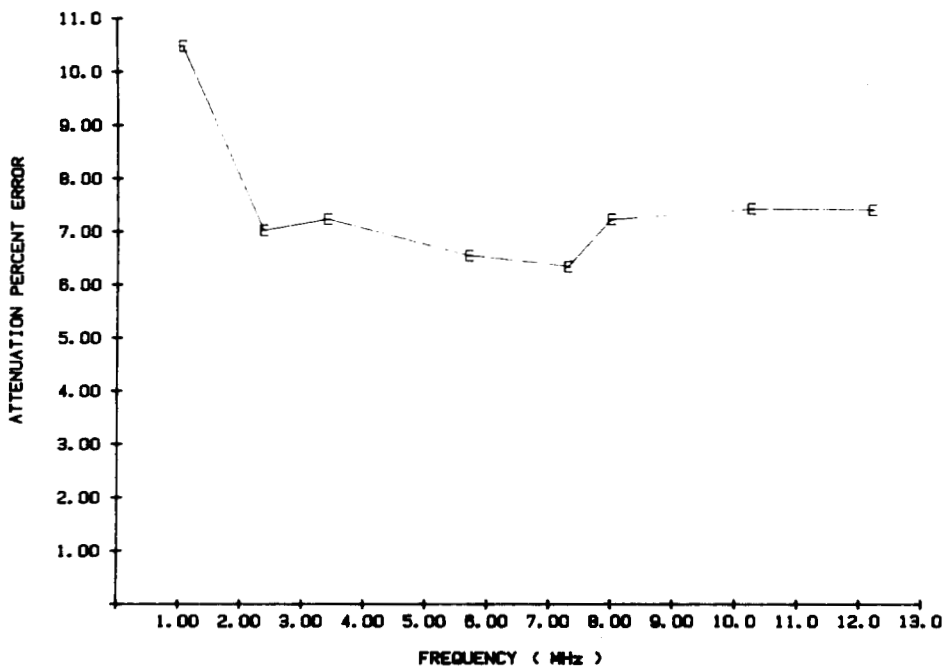
The uncertainty in sample thickness  $d$  presents an experimental challenge because soft biological samples are not rigid and may have irregular surfaces. If rigid containers are used to enforce uniform thickness, the excess reflection and attenuation effects must be accounted for. In practice, thin plastic film windows have been used with a combination of micrometer and pulse echo techniques to measure thickness, resulting in 3–6 percent typical uncertainty for 1.5-cm samples [10].

A practical use of (18) is to implement the expression with computer-controlled experimentation [10] where averaging over time and over different sample repositionings can be used to both improve accuracy of power measurements and also calculate the statistics. With this information, the estimate of attenuation and percent error can be simultaneously reported.

To illustrate typical results, Fig. 7(a) and (b) show the measured estimates of percent error, for a 1.5-cm section of calf liver, with measurements obtained at eight discrete frequencies between 1 and 13 MHz. At low frequencies, low attenuation results in a high multiplier of power error terms. At high frequencies, the transmitted power is insufficient compared to noise background, causing high uncertainty. In midrange where the product of  $2dA$  ap-



(a)



(b)

Fig. 7. Components of error in insertion loss attenuation measurements as recorded in experiments on 1.5-cm-thick slabs of calf liver. (a) Percent errors in sample thickness depth estimation and power measurements with and without sample present. Also given is square root of multiplier term inversely proportional to product of attenuation times thickness. (b) Sum of error components, showing total percent error as function of frequency.

proaches unity, the thickness uncertainty term is influential, supporting a lower bound on attenuation uncertainty.

If measurements are made with homogeneous rigid samples, with accurately known thicknesses matched to different frequency subbands ( $2dA = 1$  at each frequency), then attenuation uncertainties of three percent are achievable without further refinements of technique.

#### IV. CONCLUSION

Analysis of the pulse decay absorption technique reveals that dominant sources of error involve calibration of peak focal intensity and determination of tissue density and specific heat. A calibration procedure is introduced that relies on measurement of main lobe beam patterns

and total acoustic power. Theoretical results for a baffled piston source with apodizing lens are used to determine the contribution of sidelobes that strongly influence calibration but are generally noise contaminated. The use of Gaussian least-squares-error curve fit, with amplitude weighting to emphasize the main lobe, is useful for a restricted class of symmetric apodized, focused beams. The technique's advantages are that: 1) sharply focussed sub-millimeter beamwidths may be calibrated; 2) calibrations are obtained *in situ*, using the same thermocouple, sample, and positioning for both beam profile measurements and pulse decay measurements; and 3) the overall sensitivity of pulse decay technique to errors in beamwidth estimates  $\beta$  are minimized when  $\beta$  is used to estimate both temperature decay and peak intensity.

The sum of error terms currently results in approximately ten percent uncertainty in absorption coefficients; however, improved knowledge of tissue density and specific heat could result in 7-percent uncertainty for homogeneous tissues, without any further refinements in technique.

A similar analysis applied to insertion loss attenuation measurements shows that uncertainties of 5–10 percent are typical for 2-cm thick samples of liver. However, 3-percent errors are attainable for rigid slabs of homogeneous materials, without additional refinements.

#### ACKNOWLEDGMENT

The authors wish to thank Professor R. C. Chivers for his interest and rich input of ideas, particularly in the areas of radiation force measurements and transducer characterization. Thanks are also extended to Professor E. L. Carstensen and Professor J. G. Mottley for their helpful comments.

#### REFERENCES

- [1] S. A. Goss, R. L. Johnston, and F. Dunn, "Comprehensive compilation of empirical ultrasonic properties of mammalian tissue," *J. Acoust. Soc. Amer.*, vol. 64, no. 2, pp. 423–457, 1978.
- [2] —, "Compilation of empirical ultrasonic properties, II," *J. Acoust. Soc. Amer.*, vol. 68, no. 1, pp. 93–108, 1980.
- [3] —, "Ultrasonic absorption and attenuation in mammalian tissues," *Ultrasound Med. Biol.*, vol. 5, pp. 181–186, 1979.
- [4] P. W. Marcus and E. L. Carstensen, "Problems with absorption measurements of inhomogeneous solids," *J. Acoust. Soc. Amer.*, vol. 58, no. 6, pp. 1334–1335, 1975.
- [5] L. A. Frizzell, E. L. Carstensen, and J. D. Davis, "Ultrasonic absorption in liver tissue," *J. Acoust. Soc. Amer.*, vol. 65, no. 5, pp. 1309–1312, 1979.
- [6] S. A. Goss, J. W. Cobb, and L. A. Frizzell, "Effect of beamwidth and thermocouple size on the measurement of ultrasonic absorption using the thermoelectric technique," in *IEEE Ultrason. Symp. Proc.* New York: IEEE Press, 1977, pp. 206–211.
- [7] K. J. Parker, "The thermal pulse decay technique for measuring ultrasonic absorption coefficients," *J. Acoust. Soc. Amer.*, vol. 74, no. 5, pp. 1356–1361, 1983.

- [8] —, "Effects of heat conduction and sample size on the ultrasonic absorption measurement," *J. Acoust. Soc. Amer.*, vol. 77, no. 2, pp. 719–725, 1985.
- [9] S. A. Goss *et al.*, "Elements of tissue characterization Part II, Ultrasonic propagation parameters measurements," in *Ultrasonic Tissue Characterization II*, M. Linzer, Ed. Washington, DC: US Dep. Commerce, NBS Special Publication 525, 1979, pp. 43–51.
- [10] M. E. Lyons and K. J. Parker, "Attenuation and absorption soft tissues: II—Results," *IEEE Trans. Ultrason. Ferroelec. Freq. Contr.*, scheduled to appear.
- [11] F. Dunn, A. J. Averbuch, and W. D. O'Brien, "A primary method for the determination of ultrasonic intensity with the elastic sphere radiometer," *Acustica*, vol. 38, no. 1, pp. 58–61, 1977.
- [12] B. A. Herman and G. R. Harris, "Calibration of miniature ultrasonic receivers using a planer scanning technique," *J. Acoust. Soc. Amer.*, vol. 72, no. 5, pp. 1357–1363, 1982.
- [13] J. W. Goodman, *Introduction to Fourier Optics*. New York: McGraw-Hill, 1968.
- [14] M. Born and E. Wolf, *Principals of Optics*, 6th ed. Elmsford, NY: Pergamon, 1980.
- [15] J. D. Aindow, A. Markiewicz, and R. C. Chivers, "Quantitative investigations of disk ultrasonic sources," *J. Acoust. Soc. Amer.*, vol. 78, no. 5, pp. 1519–1529, 1985.
- [16] H. F. Bowman, E. G. Cravalho, and M. Woods, "Theory, measurement, and application of thermal properties of biomaterials," in *Annual Review of Biophysics and Bioengineering*, vol. 4, L. J. Mullens, Ed., 1975.



**Kevin J. Parker** (S'79–M'81–SM'87) was born in Rochester, NY, in 1954. He received the B.S. degree in engineering science, *summa cum laude*, from S.U.N.Y., Buffalo, in 1976, and the M.S. and Ph.D. degrees in electrical engineering and biomedical ultrasonics from M.I.T., Cambridge, in 1978 and 1981, respectively.

From 1981 to 1985 he was an Assistant Professor of Electrical Engineering at the University of Rochester; currently he holds the title of Associate Professor. His research interests are in ultrasonic tissue characterization, medical imaging, and general linear and nonlinear acoustics.

Dr. Parker was the recipient of a National Institute of General Medical Sciences Biomedical Engineering Fellowship (1979), Lilly Teaching Fellowship (1982), and Whitaker Foundation Biomedical Engineering Grant Award (1983). He serves as Chairman of the Rochester Section of the IEEE Engineering in Medicine and Biology Society, a member of the IEEE Sonics and Ultrasonics Symposium Technical Committee, and as reviewer and consultant for a number of journals and institutions. He is also a member of the Acoustical Society of America and the American Institute of Ultrasound in Medicine.



**Mark E. Lyons** was born in White Plains, NY, in 1959. He received the B.S. degree from Cornell University, Ithaca, NY, in 1981 and the M.S. degree from the University of Rochester, Rochester, NY, in 1987, both in electrical engineering.

From 1981 to 1984 he worked as a Machine Control Engineer in the Engineering Department of the Proctor and Gamble Company. He is currently working in the research area of the Xerox Corporation.